THE REALIZATION AND THE DISSEMINATION OF THE DETECTOR-BASED KELVIN

Howard W. Yoon, Charles E. Gibson, David W. Allen, Robert D. Saunders, Maritoni Litorja, Steven W. Brown, George P. Eppeldauer, Keith R. Lykke

Optical Technology Division
National Institute of Standards and Technology
Gaithersburg, MD 20899
USA

ABSTRACT

In the International Temperature Scale of 1990 (ITS-90), temperatures above the freezing temperature of silver are determined with radiation thermometers calibrated using spectral radiance ratios to one of the Ag-, Au- or Cu-freezing temperature blackbodies and the Planck radiance law. However, due to the use of spectral radiance rats, the temperature uncertainties of the ITS-90 increase as the square of the temperature ratios. Recent acoustic-gas thermometry measurements have also shown that the underlying thermodynamic temperatures used in the radiance ratios in determining the Ag- and Au-fixed point temperatures could be in error. Since the establishment of ITS-90, much progress has been made in the development of radiation thermometers and blackbody sources. Cryogenic electrical-substitution radiometry is widely used in detector and radiometer calibrations, and stable, high-temperature metal-carbon eutectic blackbodies are under development. Radiation thermometers can be calibrated for absolute radiance responsivity, and blackbody temperatures determined from measurement of optical power without the use of any fixed points thus making possible direct dissemination of thermodynamic temperatures. We show that these temperatures can be measured with lower final uncertainties than the ITS-90 derived temperatures. We have shown that these "Absolute Pyrometers" can be used to determine the thermodynamic temperatures of the ITS-90 fixed points as well as also being used in bilateral comparisons of temperature scales. Many leading national measurement institutes are already utilizing detector-based temperatures in establishing spectroradiometric source scales. We believe, that due to these developments, the international temperature scale should be revised so that a thermodynamic temperature scale can be directly disseminated.

1. INTRODUCTION

The development of an international temperature scale and the periodic adjustments of the scale are attempts to disseminate and best reproduce thermodynamic temperatures. Thermodynamic temperatures can be determined by primary thermometry using equations of state that relate temperatures with measurable quantities without any temperature-dependent parameters; examples are pressure-volume and acoustic gas thermometry, noise thermometry and detector-based radiation thermometry [1]. Due to the difficulties in developing facilities and performing experiments for primary thermometry, various phase transitions of material have been assigned temperatures based upon available thermodynamic temperature measurements, and these fixed-points cells and blackbodies are in-turn used to calibrate secondary thermometers or sensors whose output changes in response to temperature. Almost all the national measurement institutes (NMI) rely upon a set of these fixed-points to generate the international temperature scale instead of performing their own primary thermometry. Thus, the current International Temperature Scale of 1990 (ITS-90), with its system of fixed-points and defining instruments, is an attempt at achieving closest agreement with the thermodynamic temperature scale [2].

Although there are no fundamental, inherent temperature limitations in the equations describing the relationship between measurables and thermodynamic temperatures in primary thermometry, in practice, experimental concerns limit these primary thermometers to a range of temperatures. Since

the experimental upper temperature limit for the lowest uncertainty constant-volume gas thermometry and acoustic-gas thermometry is < 900 K, these temperature limitations have impacted the higher temperature uncertainties of the ITS-90 [3]. Due to the conflicting results of two constant-volume gas thermometry measurements, the mean of the two results were used as reference values at 743 K for radiation thermometry in determining the Al-, Ag- and Au-freezing temperatures used in the ITS-90 [1]. The latest acoustic-gas thermometry measurements have been found to be consistent with the work of Edsinger and Schooley, and this implies that the current ITS-90 assignments for the each of the high-temperature fixed-points have inherent temperature biases [4]. There have also been recent efforts in noise-thermometry in measurements of the Ag- and Pd-freezing temperatures, but the uncertainties of the noise-thermometry determinations are comparable to those assigned to the ITS-90 values of these fixed points [5]. Even with new efforts in noise thermometry using super-conducting junctions to generate noise standards, the thermodynamic temperature uncertainties above the Ag-point are not expected to be greatly reduced below the present uncertainties [6].

Detector-based radiation thermometry can used for thermodynamic temperature determinations which are applicable over a wide range of temperatures from 60 K to > 3000 K. With the development of cryogenic electrical substitution radiometers (ESR), accurate measurements of optical power by comparison to electrical power resulted in the determinations of the Stefan-Boltzmann constant from total radiation thermometry [7]. As the temperatures of blackbodies are increased, spectrally-selective radiation thermometers calibrated using ESR-based radiometry can be used to determine the thermodynamic temperatures with low uncertainties using Si-diode based radiation thermometers [8]. Recognizing that these detector-based radiation thermometers be used to obtain lower temperature uncertainties than ITS-90 based radiation thermometers, many leading NMIs have developed calibration facilities for detector-based temperatures [9]. The needs for the lowest uncertainties in temperature > 900 K arise chiefly from the spectroradiometric and the photometric community where sources with relative spectral distributions similar to 3000 K blackbody sources are required.

With the development of high-temperature metal-carbon and metal carbide-carbon eutectics, these stable sources can be used as fixed points for redefinition of the ITS [10]. However, for the lowest thermodynamic uncertainties needed for the scale, detector-based radiation thermometry should be used to determine the transition temperatures of the eutectics in order to determine the thermodynamic temperatures.

Although detector-based radiation thermometry is increasingly being used in the international radiometric community, the international temperature community still utilizes the source-based ITS-90 derived temperatures, leading to a possible inconsistency in the disseminated radiometric and temperature scales from a common NMI. The situation is analogous to that in photometry with the transition from the platinum-point based candela to the redefinition of the candela based upon optical power in 1979 [11]. If a general redefinition of the ITS-90 over all temperatures is not feasible or needed at the present time, then the ITS-90 above the Ag-point, or perhaps above the Al-point, should be redefined to reflect the maturity of detector-based radiation thermometry.

In this paper, we describe the facilities and the experimental procedures in calibrating a detector-based radiation thermometer traceable to a cryogenic electrical substitution radiometer. The radiation thermometer, Absolute Pyrometer 1 (AP1), has been constructed at NIST to be temporally stable and is characterized for linearity, size-of-source effect (SSE) and detector-based radiance responsivity. The AP1 was used to determine the thermodynamic temperatures of the Ag- and Au-freezing temperatures and was also used for a bilateral comparison of temperature scales with the National Physical Laboratory (NPL), United Kingdom, using high-temperature metal-carbon eutectic blackbodies. With these measurements, we demonstrate that primary thermometers such as the AP1 can be used to directly disseminate thermodynamic temperatures with lower uncertainties than any ITS-90 based thermometer. We describe improvements to radiation thermometer designs to reduce the SSE to $< 5 \times 10^{-5}$ and improve the long-term stability of the responsivity from the use of graphite or

invar reference rods in the construction. We believe that these results along with further advances at other NMIs will result in the practical adoption of detector-based thermodynamic temperature scale above the Ag-freezing temperature with possible extension down to the Al-freezing temperature.

2. DETECTOR-BASED RADIANCE RESPONSIVITY CALIBRATIONS

Without the development of facilities to derive radiance and irradiance responsivity from electrical substitution radiometers, detector-based radiation thermometry would not be possible [12]. Radiation thermometers can be constructed to measure irradiance or radiance, and simple filter radiometers with a precision aperture can be used to measure the irradiance of the source if the source also has a defining aperture. If the spatial uniformity of the filter radiometer is quantified, then power responsivity measurements along with the aperture area will provide the irradiance responsivity. However, typical radiation thermometers are constructed using lenses or mirrors to define a target area to measure in radiance mode, and blackbody temperatures can be determined using the detector-based radiance responsivities and Planck's law by the use of

$$i_c = \int S_L \cdot \varepsilon \cdot L(\lambda, T)\, d\lambda \,, \tag{1}$$

where i_c is the calculated photocurrent for temperature, T, S_L is the radiance responsivity, $L(\lambda, T)$ is the Planck radiance law, and ε is the emissivity of the blackbody. With the use Eq. 1, blackbody temperatures can be determined directly with no adjustable parameters in the measurement equation relating the radiance responsivity to the thermodynamic temperature. Since there is a unique relationship between the calculated current and the blackbody temperatures in Eq. 1, then integrations can be performed to find a match between the calculated and the measured photocurrents to determine blackbody temperatures.

At NIST, the radiance and irradiance responsivities of radiometers are calibrated using the NIST Spectral Irradiance and Radiance responsivity Calibrations using Uniform Sources (SIRCUS) facility [13]. Briefly, the 6-element Si-trap detectors with precision apertures used in this facility are calibrated for power responsivity using the NIST High-Accuracy Cryogenic Radiometer (HACR) [14], and from the knowledge of the spatial uniformity and the aperture area of the trap detectors [15], the detector-based spectral irradiance responsivity is determined as shown in Fig. 1.

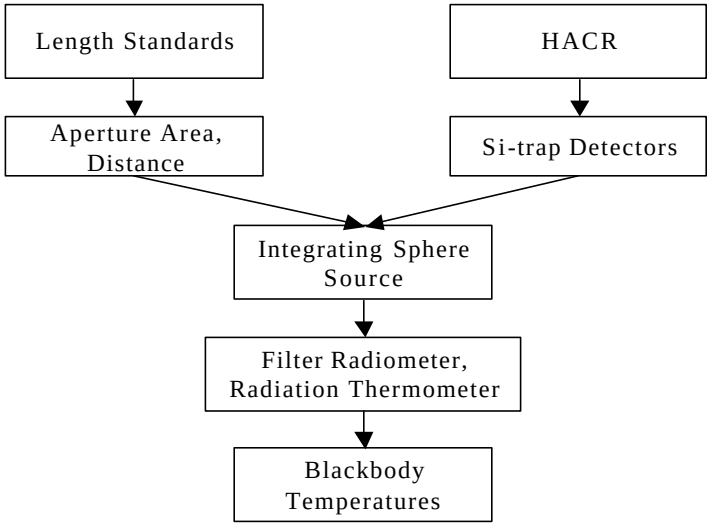

Figure 1. The realization chain for thermodynamic temperatures based upon detector-based radiation thermometry.

With the irradiance responsivity of the Si-trap detectors calibrated from the power responsivity, the spectral irradiance of the laser-illuminated integrating sphere source (ISS) can be determined. Knowing the distance between the Si-trap detector aperture and the precision aperture of the ISS determines the detector-based spectral radiance of the ISS. The above procedure is repeated with changing laser wavelengths, and thus the radiance or the irradiance responsivity of the filter radiometer or the radiation thermometer can be determined. Since the radiation thermometer is calibrated as a system, knowledge of the lens transmittances is not needed, and complex radiation thermometers with many optical elements can also be calibrated in the SIRCUS facility.

3. THE DESIGN AND CHARACTERIZATION OF THE AP1

With very few exceptions, the performances of commercial radiation thermometers are quite limited in the temporal stability, size-of-source and optical imaging so that custom radiation thermometers are required. A schematic of the AP1 in front of the gold-point blackbody is shown in Fig. 2. The dimension of the AP1 from outside of the front plate to the back plate is 53 cm. The optical elements are attached to three 50 cm long, 12.5 mm diameter invar rods for stability. A gradient-index singlet lens is chosen for the objective to minimize the possible scattered light from the lens interfaces and to improve the image quality. The objective distance is set at 50 cm using a fixed-focus singlet lens with

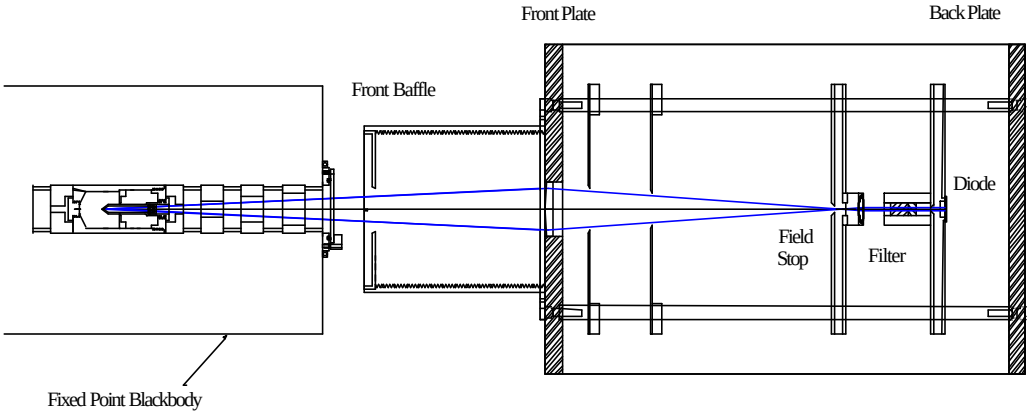

Figure 2. The schematic of the AP1 in front of the gold-point blackbody.

an image distance of 33.3 cm. A 0.5 mm diameter, blackened bi-metal pinhole is used as the field stop, which results in a nominal target size of 0.75 mm diameter. The size of the target area was chosen such that tungsten-strip lamps and fixed-point blackbodies could be used in comparison to variable-temperature blackbodies with larger cavity apertures.

An achromatic lens collimates the light after the field stop. The collimated light passes through the interference filter and is incident on the 5.8 mm by 5.8 mm square Si photodiode. The spot size on the diode is estimated to be 5 mm diameter from ray-trace analysis. The spectral selection is performed using an ion-assisted deposited interference filter with center wavelength at 650 nm. The spectral selection filter is temperature stabilized near room temperature, and the hermetically sealed Si photodiode has a 2-stage thermo-electric cooler for operation at −15 °C to achieve a noise-equivalent power of 10 fW. The entire pyrometer can be purged with dry air or nitrogen to reduce effects due to humidity on the optical elements.

3.1 RADIANCE RESPONSIVITY CALIBRATION OF THE AP1

The AP1 was calibrated for radiance responsivity using the NIST SIRCUS facility. The detector-based radiance responsivity of the AP1 is shown in Fig. 3. The interference filter used in the AP1 has $< 1x10^{-7}$ suppression in the out-of-band region from the peak value of the responsivity. The full-width at half-maximum (FWHM) of the radiance responsivity is 10 nm. The calibration of the detector-based radiance responsivity is performed with the AP1 as a system and thus any other radiation thermometer can be calibrated similarly. The total expanded uncertainty of the radiance responsivity is 0.15 % (k = 2).

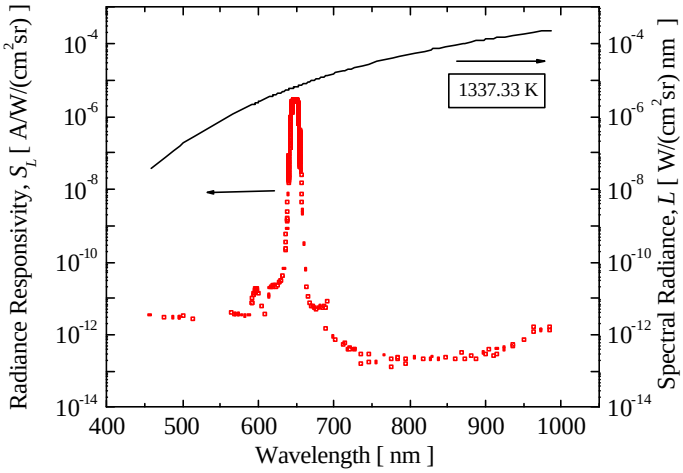

Figure 3. The radiance responsivity of the AP1 measured in the SIRCUS facility plotted with the Planck radiance at 1337.33 K. The center wavelength is 650 nm with a FWHM of 10 nm. The out-of-band suppression of $< 1x10^{-7}$ is achieved in the wavelength region from 700 nm to 1000 nm.

3.2 DETERMINATION OF DETECTOR-BASED TEMPERATURES

The calculated photocurrents from the use of Eq. 1 and the responsivity in Fig. 3 are plotted versus the respective blackbody temperatures in Fig. 4 and shows that the photocurrents range from $< 10^{-10}$ A to

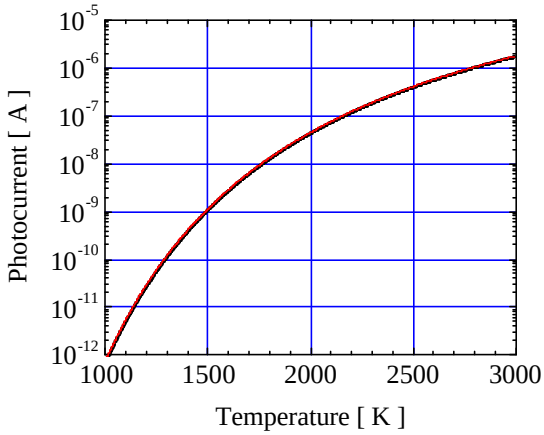

Figure 4. The calculated photocurrent from the use of Eq. 1 with emissivity of 1. The temperature of the blackbody is determined using the relationship between the calculated photocurrent and the temperature.

$> 10^{-6}$ A as the blackbody temperatures increase from the Ag- and Au-point temperatures to 3000 K. The range in photocurrent from the Ag-freezing temperature to > 3000 K is in the linear photocurrent region for Si diodes if the radiation is not incident on the edges of the photodiode [16]. The photocurrent of $< 10^{-10}$ A near the Ag-freezing temperatures indicates the need for low noise photodiodes and preamplifiers for these measurements.

3.3 LINEARITY CHARACTERIZATION OF THE AP1

The measurement of the radiance responsivity was performed in SIRCUS using 10^8 V/A as shown in Table 1, and the normalization factors to the other gains are needed if the AP1 is used at different gain settings. Instead of the traditional determination of radiometer linearity using radiation sources, the preamplifier was measured separately with a programmable constant-current source and compared to the current-to-voltage conversions using the NIST Precision Preamplifier (NPP). The NPP is a current meter whose nominal decade values of the feedback resistors have a tolerance of 0.01 %. The temperature coefficients of the resistances are 10×10^{-6}/ °C. The AP1 preamplifier was calibrated against the NPP using an input-current on/off switch to eliminate the output offset voltages of the test and standard preamplifiers. As the noise and ripple pickup was minimized in the preamplifier standard, the test preamplifier could be calibrated with 0.022 % ($k = 2$) uncertainty, even at 10^{10} V/A.

Table 1. AP1 preamplifier gains determined by reference to NIST Precision Preamplifier with 0.01 % precision resistors used as feedback resistors.

Gain	Gain factors [V/A]	Uncertainty ($k = 2$) [%]	Ratios	Normalization factors to gain 10^8
6	1.00010E+06	0.02	$10^8/10^6$ =	9.95920E+01
7	1.00008E+07	0.014	$10^8/10^7$ =	9.95940E+00
8	9.96020E+07	0.014	$10^8/10^8$ =	1.00000E+00
9	9.94820E+08	0.022	$10^8/10^9$ =	1.00121E-01
10	9.94330E+09	0.022	$10^8/10^{10}$ =	1.00170E-02

4. DETERMINATION OF THE Ag- AND Au-FREEZING TEMPERATURES

One of the most critical tests of the detector-based radiation thermometer is the comparison of the thermodynamic temperatures of the Ag- and Au-freezing temperatures to the ITS-90 [17]. If the detector-based measurements are not within the combined uncertainties of the experiment, then some unknown systematic effect could be improperly characterized. The AP1 was used to compare the thermodynamic Ag- and Au-freezing temperatures to the ITS-90 assigned values [3]. A summary of the measurements is listed in Table 2.

Table 2. Summary of the Ag- and Au-freezing temperature determinations with the ITS-90 assignments.

Freezing Material	T (AP1) [K]	Uncertainty T (AP1) [K] ($k = 2$)	T_{90} [K]	Uncertainty T (ITS-90) [K] (k=2)	T-T_{90} [K]
Ag	1234.956	0.106	1234.93	0.080	0.026
Au	1337.344	0.121	1337.33	0.100	0.014

From Table 2, the dominant uncertainty component is from the radiance responsivity uncertainty of 0.15 % ($k = 2$) which corresponds to an expanded temperature uncertainty of 0.121 K and 0.106 K at the Ag- and Au-freezing temperatures, respectively. Since the center wavelength of the AP1 is in the wavelength and temperature region where the Wien approximation is applicable, the uncertainty of the temperature from the uncertainty of radiance is found from the derivative of the Wien approximation, and the differences, T-T_{90}, are found to be within the combined uncertainties.

5. COMPARISON OF NPL ITS-90 AND NIST THERMODYNAMIC TEMPERATURES

The NIST thermodynamic temperature scale based on the AP1 was also used for a bi-lateral comparison of temperature scales with the NPL using a set of metal-carbon eutectic blackbodies [18]. The temperatures of the eutectics were assigned at the NPL on ITS-90 and then compared by transporting the crucibles to NIST for measurements with the AP1. The results are shown Fig. 5. The solid lines are the combined uncertainties of the measurements and the dotted lines are the uncertainties of the AP1 measurements. The differences are within the combined uncertainties of the comparison and within the uncertainties of the detector-based temperatures as well. The uncertainties of the NIST detector-based temperature scale is about half of those on the ITS-90 based scale of NPL.

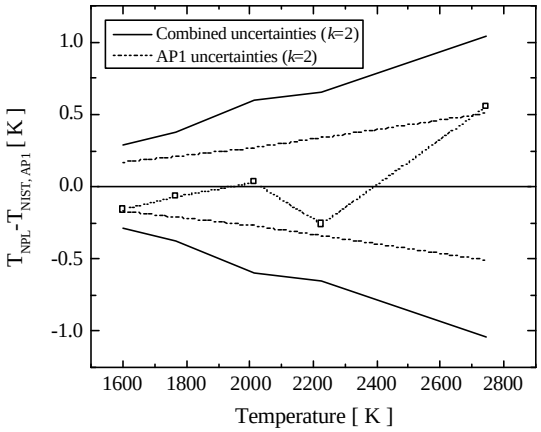

Figure 5. The differences between the NPL (ITS-90) assigned temperatures and the NIST thermodynamic temperatures of the metal-carbon eutectics. The solid line is the combined temperature uncertainties and the dotted line denotes only the AP1 uncertainties.

6. NEW DESIGNS FOR RADIATION THERMOMETERS

Our experience with the AP1 and further analysis of the contributions to the SSE in radiation thermometers have lead to new designs for future NIST radiation thermometers. These radiometers will be used for detector-based radiation thermometry and for ratio radiation thermometry to obtain temperatures to the Sn-point with the lowest uncertainties. A design to be used for detector-based radiation thermometry from 350 nm to 2500 nm utilizing different detectors, filters and lenses is shown in Fig. 6. The outer case is constructed with 25 cm diameter anodized aluminum, and the large outer case is for suppression of scatter from internal reflections. The internal walls are covered with low-reflective black appliqué, and the field stop is tilted by 10° to avoid direct reflections back onto the objective lens. For temporal stability, the optical elements are attached to graphite or invar reference rods which have low coefficients of thermal expansion. The radiometer is also designed for removal of the objective lens from the outside for easy cleaning and replacement if the objective lens becomes damaged. Our goal for the uncertainty due to long-term stability of the radiance responsivity is 0.01 % or 100 ppm.

The optical design of the radiometer has been influenced by our studies of the contributions to the SSE [19]. The main source of the SSE in the NIST design has been determined to be the scatter from

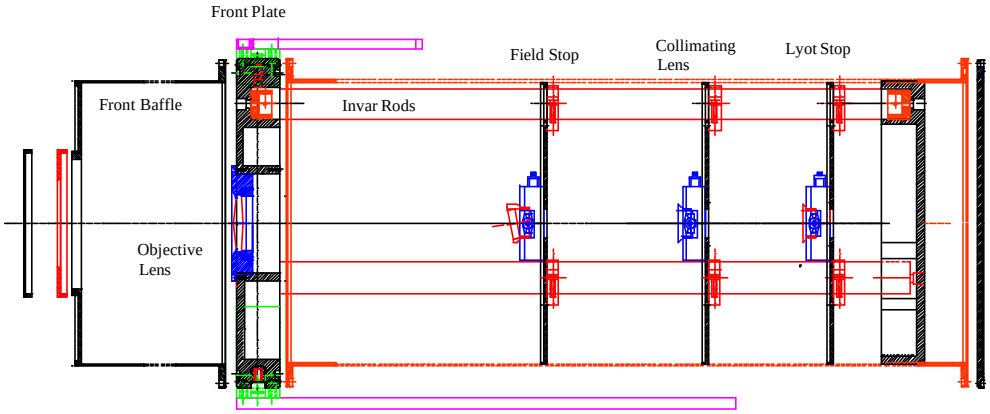

Figure 6. A side-view schematic of the Invar-rod referenced radiation thermometer. The outer diameter of the radiation thermometer is 25 cm.

the objective lens. The scatter can be reduced by the placement of the Lyot stop or the aperture stop behind the field stop such that the image of the objective lens is formed on the Lyot stop by the collimating lens. The optical imaging and chromatic aberrations have been assessed for various different types of lenses using a commercial optical modeling software. We have found that for radiation thermometry, the simplest objective lens design leads to the lowest SSE as shown in Fig. 7. In Figure 7, the optical design utilized in the NIST radiation thermometers is compared against the SSE [20] from the Linear Pyrometer 3 (LP3)*, a common radiation thermometer used at NMIs. The simpler objective lens can lead to > 10 reduction in the SSE. Custom lens designs are being assessed to obtain both optical performance as well as low surface scatter.

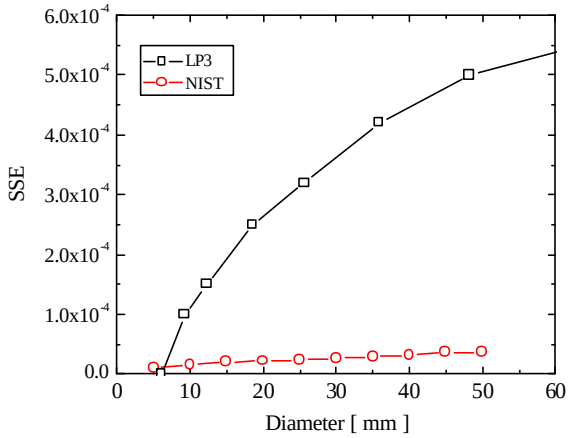

Figure 7. A comparison of the SSE between the NIST radiation thermometer design and the LP3.

8. THE DEVELOPMENT OF A FUTURE TEMPERATURE SCALE

One of the dominant factors in the increase in the ITS-90 temperature uncertainties above the Ag-freezing point is the lack of higher-temperature fixed points above 1400 K. Recent developments in high-temperature metal-carbon and metal-carbide-carbon eutectic blackbodies will lead to lower temperature uncertainties if the eutectic blackbodies are determined to be suitable for use as high temperature fixed-points [21]. Spectral radiances of the new metal- carbon and metal carbide-carbon eutectic blackbodies are shown along with the Au- and the Ag-fixed points in Fig. 8. For any future temperature scale to be a good representation of thermodynamic temperatures, the temperatures of the high temperature eutectic blackbodies must be determined using absolute detector-based techniques. If radiance ratios from the Au-point temperature are used to determine the temperatures of the eutectics then the uncertainties would be unacceptably large, since the uncertainties are found by using

$$u(T_{\mathrm{BB}}) = \frac{u(T_{\mathrm{REF}})}{T_{\mathrm{REF}}^2} T_{\mathrm{BB}}^2 , \qquad (2)$$

with T_{REF} denoting the fixed point blackbody, and T_{BB} the unknown temperature of the eutectic-point blackbody.

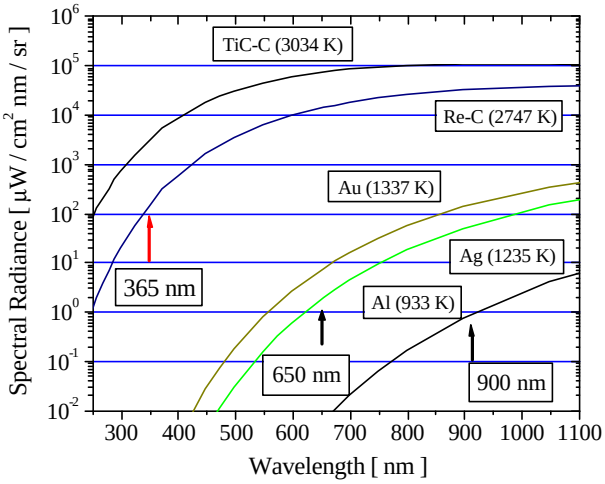

Figure 8. The spectral radiances of the blackbodies at the respective temperatures. The measurements of the Au- and the Ag-freezing points at 650 nm are compared with the planned measurements of the eutectic points at shorter wavelengths.

However, there is still a role for ratio radiometry in the new temperature scale. If the temperature of the reference fixed-point blackbody described in Eq. 2 is greater than the temperatures of the blackbodies under measurement, then the temperature uncertainties of the lower temperature blackbodies become smaller by the ratio of the squares of the respective temperatures. A possible future temperature scale could be based upon an absolute temperature determination of several high-temperature metal-carbon eutectic blackbodies ~ 3000 K with the temperatures of the lower-temperature fixed point determined using radiance ratios.

Table 5 shows the temperature uncertainties both using absolute detector-based techniques and radiance ratios to the TiC-C blackbody, and the uncertainties of the detector-based temperature determinations can be estimated from the derivative of the Wien approximation to Planck's radiance law,

$$\frac{\Delta L}{L} = \frac{c_2}{l}\frac{\Delta T}{T^2}, \tag{3}$$

which shows the relationship between the uncertainty in radiance, L, to the uncertainty in blackbody temperature, T, where c_2 is the second Planck's constant, and l is the wavelength. If the temperatures of the respective blackbodies are measured at the wavelengths shown in Col. 3, then the radiance uncertainties shown in Col. 4 lead to the uncertainties in Col. 5 as found using Eq. 3. However, if the temperatures of the lower temperature fixed points are determined using radiance ratios to the TiC-C, then the temperature uncertainties decrease as in Eq. 2 thus leading to lower uncertainties as shown in Col. 6. For the lowest uncertainties in the temperature scale, both types of temperature determinations are needed to verify the assigned uncertainties in addition to the ratio radiometry based on the lower-temperature acoustic-gas thermometry.

Table 5. A comparison of the temperature uncertainties found using absolute detector-based techniques and radiance ratios.

Material	Temperature (K)	Wavelength (nm)	Radiance Uncertainty (%) (k = 2)	Detector-based Temperature Uncertainty (K) (k = 2)	Ratio to TiC-C Ratio Pyrometry (K) (k = 2)
TiC-C	3034	365	0.1	0.234	---
Re-C	2748	400	0.1	0.210	0.172
Cu	1357.77	650	0.1	0.083	0.042
Au	1337.33	650	0.1	0.081	0.041
Ag	1234.93	800	0.1	0.069	0.035
Al	933.473	900	0.1	0.055	0.020
Zn	692.677	1250	0.3	0.125	0.011

9. DISCUSSION

With the improvements in radiation thermometer designs for long-term stability and low SSE, the total radiance responsivity uncertainty in detector-based thermometry is expected to decrease to 0.1 % (k = 2) in the wavelength region from 350 nm to 1000 nm. Although, even with the current design of the AP1, the detector-based determinations of the Ag- and Au-freezing temperature are in agreement with the combined uncertainties, further reduced uncertainties will lead to the thermodynamic uncertainties as shown in Table 6. The present thermodynamic uncertainties in the ITS-90 assigned temperatures are listed [3]. Although the uncertainties appear comparable, the limiting uncertainties in noise-thermometry are due to random (Type A) uncertainties, while the dominant uncertainties in detector-based thermometry are due to systematic (Type B) uncertainties, indicating that even lower total uncertainties are achievable with detector-based thermometry.

Table 6. A comparison of the thermodynamic temperature uncertainties obtained using noise and detector-based thermometry with the current uncertainties in the ITS-90 assignments. The detector-based thermometry is determined using 0.1 % (k = 2) uncertainty in the radiance responsivity at 650 nm.

Metal	T_{90} [K]	T_{90}, Thermodynamic temperature uncertainty [mK] (k = 2)	Noise thermometry uncertainty [mK] (k = 2)	Detector-based thermometry uncertainties [mK] (k = 2)
Al	933.473	50	–	55
Ag	1234.93	80	80	68
Au	1337.33	100	–	81
Cu	1357.77	120	126	83
Pd	1827.95	200	212	151

We have shown that detector-based thermometry can achieve comparable uncertainties to the ITS-90 uncertainties near the Ag- and Au-freezing temperatures and can attain lower uncertainties than any ITS-90 based radiation thermometry at higher temperatures. The promise of lower uncertainties and the requirements for determining the metal-carbon eutectic transitions with the lowest uncertainties have led to efforts at many NMIs to set up similar detector-based radiance responsivity calibration facilities, and with such facilities, direct disseminations of thermodynamic temperatures are possible with either calibrated radiation thermometers or secondary transfer standard sources.

We believe that these developments will lead to a reassessment of the ITS-90 and the future international temperature scale. Since it is possible, with detector-based radiation thermometry, to directly disseminate thermodynamic temperatures, the present Ag-, Au-, Cu- and even the Al-freezing points will not remain as fixed points but will be allowed to vary within the uncertainty of the thermodynamic temperature determinations. Remaining within the framework of ITS-90 could result in higher temperature uncertainties than is possible with a detector-based scale, and NIST has already recognized the restrictions that a fixed-point scale places upon the temperature uncertainties. The current situation is analogous to the time-period when the International Practical Temperature Scale of 1968 (IPTS-68) was utilized prior to ITS-90. Although the deviations from the thermodynamic temperature scale of the IPTS-68 were recognized, restrictions of a fixed-point based scale meant that the discrepancies could not be resolved without new temperatures assigned to the fixed points. Recognizing these restrictions, NIST's radiation thermometry has been detector-based since 1990 with a separate, independent, thermodynamic temperature determination of the Au-freezing temperature [22], and with the new generation of radiation thermometers, will soon be completely detector-based. If the ITS-90 scale is desired, then correction factors can be applied to the NIST detector-based scale for international comparisons and to comply with mutual recognition arrangements.

10. CONCLUSION

Much progress has been made toward an implementation of a detector-based thermodynamic temperature scale with the development of SIRCUS, aperture-area measurement facility and optimized radiation thermometers. The impetus for such progress has arisen from the spectroradiometric community and the need for the lowest-uncertainty temperature measurements of the new metal-carbon eutectic blackbodies. We have shown that these detector-based primary radiation thermometers can be used to determine the Ag- and Au-freezing temperatures and even for bilateral comparisons of temperature scales. With continuing efforts at many different NMIs, direct dissemination of thermodynamic temperatures will be possible in the near future. We believe that a reassessment of the ITS-90 is needed to reflect the developments in detector-based radiation thermometry.

ACKNOWLEDGMENTS

The authors gratefully acknowledge discussions with Weston Tew, Greg Strouse and Dean Ripple of the Process Measurements Division at NIST on various aspects of noise- and acoustic-gas thermometry.

REFERENCES

***** Certain commercial equipment, instruments, or materials are identified in this paper to foster understanding. Such identification does not imply recommendation or endorsement by the National Institute of Standards and Technology, nor does it imply that the material or equipment are necessarily the best available for the purpose.

[1] Quinn T. J., Temperature, 2 nd ed., London, Academic Press Ltd., 1990.
[2] Preston-Thomas H., "The International Temperature Scale of 1990 (ITS-90)", *Metrologia* **27**, 1990, pp. 3-10.
[3] Ref [1] pp. 56-57.
[4] Strouse G. F., Defibaugh D. R., Moldover M. R., Ripple D. C., "Progress in primary acoustic thermometry at NIST: 273 K to 505 K", *Temperature: Its Measurement and Control in Science and Industry, Vol. 7*, edited by D. C. Ripple, 2003, pp. 31-36.
[5] Edler F., Kühne M., Tegeler E., "Noise Thermometry above 960 °C", *Proceedings of TEMPMEKO 1999*, Delft, edited by Dubbeldam J. F., de Groot, M. J., 1999, pp. 394 -399.
[6] Nam S. W., Benz S. P., Martinis J. M., Dresselhaus P., Tew W. L., White D. R., "A Ratiometric Method for Johnson Noise Thermometry Using a Quantized Voltage Noise Source", *Temperature: Its Measurement and Control in Science and Industry, Vol. 7*, edited by D. C. Ripple, 2003, pp. 37 -42.
[7] Quinn T. J., Martin, J. E., "A radiometric determination of the Stefan-Boltzmann constant and thermodynamic temperatures between -40 °C and +100 °C", *Philosophical Transactions of the Royal Society of London* **A 316,** 1985, pp. 85 -189.
[8] Allen D. W., Saunders R. D., Johnson B. C., Gibson C. E., Yoon H. W., "The Development and Characterization of an Absolute Pyrometer Calibrated for Radiance Responsivity", *Temperature: Its Measurement and Control in Science and Industry, Vol. 7*, edited by D. C. Ripple, 2003, pp. 577 -582
[9] Fox N. P., *Metrologia* **32,** 1995/1996, pp. 535 -543.; Taubert D. R., Hartmann J., Hollandt J., Fischer J., "Investigation of the Accuracy of the ITS-90 with Reference to Thermodynamic Temperature in the Range from 400 °C up to 600 °C", *TMCSI*, Vol. 7, Chicago, edited by Ripple D. C., 2003, pp. 7 –12.
[10] Yamada Y., Sakate H., Sakuma F., Ono A., "A Possibility of Practical High Temperature Fixed Points above the Copper Point, *Proceedings of TEMPMEKO1999*, Delft, edited by Dubbeldam J. F., de Groot, M. J., 1999, pp. 535 -540.
[11] Blevin W. R., and Steiner B., "Redefinition of the Candela and Lumen", *Metrologia* **11**, 1975, pp. 97-104.
[12] Ref 9.
[13] Brown S. W., Eppeldauer G. P., Lykke K. R., "NIST Facility for Spectral Irradiance and Radiance Responsivity Calibrations with Uniform Sources", *Metrologia* **37**, 2000, pp. 579-582.
[14] Gentile T. R., Houston J. M., Cromer C. L., "National Institute of Standards and Technology High-accuracy Cryogenic Radiometer", *Appl. Opt.* **35**, 1996, pp. 4392-4403.
[15] Fowler J. and Litorja M., "Geometric Area Measurements of Circular Apertures for Radiometry at NIST", *Metrologia* **40**, 2003, pp. S9-S12.
[16] Battuello M., Bloembergen P., Girard F., Ricolfi, "A Comparison of Two Methods for Measuring the Nonlinearity of Infrared Radiation Thermometers", *Temperature: Its Measurement and Control in Science and Industry, Vol. 7*, edited by D. C. Ripple, 2003, pp. 613-618.
[17] Yoon H. W., Allen D. W., Gibson C. E., Litorja M., Saunders R. D., Brown S. W., Eppeldauer G. P., Lykke K. R., "Temperature Determination of the Ag- and Au-freezing points using a Detector-based Radiation Thermometer", submitted to the *Proceedings of Tempmeko 2004*, Croatia, 2004.
[18] Machin G., Gibson C. E., Low D., Allen D.W., Yoon H.W., "A Comparison of ITS-90 and Detector-based Scales between NPL and NIST Using Metal-carbon Eutectics ", submitted to the *Proceedings of Tempmeko 2004*, Croatia, 2004.
[19] Yoon H.W., Allen D.W. Saunders R.D., "Methods to reduce the size-of-source effect in radiation thermometers", submitted to the *Proceedings of Tempmeko 2004*, Croatia, 2004.
[20] Bloembergen P., Yamada Y., "The Impact of the Size-of_source effect on the Uncertainty of t Fixed-point Radiance Temperatures: A Case Study", submitted to the *Proceedings of Tempmeko 2004*, Croatia, 2004.
[22] Bloembergen P., Yamada Y., Yamamoto N., Hartmann J., "Realizing the High-temperature Part of a Future ITS with the Aid of Eutectic Metal-Carbon Fixed Points", *Temperature: Its Measurement and Control in Science and Industry, Vol. 7*, edited by D. C. Ripple, 2003, pp. 291-296.
[22] Mielenz K. D., Saunders R. D., Shumaker J. B., "Spectroradiometric Determination of the Freezing Temperature of Gold", *J. Res. Natl. Inst. Stand. Technol.* 95, 1990, pp. 45-67.

Address of the Principal Author: Howard W. Yoon, Optical Technology Division, NIST, 100 Bureau Drive Gaithersburg, MD 20899-8441, USA, tel. (301) 610-0094, fax (301) 869-5700, e-mail: **hyoon@nist.gov**